ARMY RESEARCH LABORATORY

Propagation of Narrow Bandwidth Wavelength Radiation Through the Atmosphere

by David Voelz, Xifeng Xiao, Prabu Adepu, and Joseph Montoya

ARL-CR-0611 **August 2008**

NOTICES

Disclaimers

The findings in this report are not to be construed as an official Department of the Army position unless so designated by other authorized documents.

Citation of manufacturer's or trade names does not constitute an official endorsement or approval of the use thereof.

Destroy this report when it is no longer needed. Do not return it to the originator.

Army Research Laboratory
White Sands Missile Range, NM 88002-5513

ARL-CR-0611 **August 2008**

Propagation of Narrow Bandwidth Wavelength Radiation Through the Atmosphere

Joseph Montoya
Survivability/Lethality Analysis Directorate, ARL

David Voelz, Xifeng Xiao, and S. Prabu Adepuand
Klipsch School of Electrical and Computer Engineering

Prepared for:
Survivability/Lethality Analysis Directorate, ARL
White Sands Missile Range, NM

Prepared by:
Klipsch School of Electrical and Computer Engineering
New Mexico State University, Las Cruces, NM

REPORT DOCUMENTATION PAGE

Form Approved
OMB No. 0704-0188

1. REPORT DATE *(DD-MM-YYYY)*	2. REPORT TYPE	3. DATES COVERED (From - To)
August 2008	Final	

4. TITLE AND SUBTITLE
Propagation of Narrow Bandwidth Wavelength Radiation Through the Atmosphere

5a. CONTRACT NUMBER
DATM05-01-C-0026

5b. GRANT NUMBER

5c. PROGRAM ELEMENT NUMBER

6. AUTHOR(S)
David Voelz, Xifeng Xiao, S. Prabu Adepu, and Joseph Montoya

5d. PROJECT NUMBER

5e. TASK NUMBER
057

5f. WORK UNIT NUMBER

7. PERFORMING ORGANIZATION NAME(S) AND ADDRESS(ES)
Klipsch School of Electrical and Computer Engineering
P.O. Box 30001, MSC 3-0
New Mexico State University
Las Cruces, NM 88003

8. PERFORMING ORGANIZATION REPORT NUMBER
ARL-CR-0611

9. SPONSORING/MONITORING AGENCY NAME(S) AND ADDRESS(ES)
U.S. Army Research Laboratory
Survivability/Lethality Analysis Directorate
ATTN: AMSRD-ARL-SL-EG
White Sands Missile Range, NM 88002-5513

10. SPONSOR/MONITOR'S ACRONYM(S)

11. SPONSOR/MONITOR'S REPORT NUMBER(S)
ARL-CR-0611

12. DISTRIBUTION/AVAILABILITY STATEMENT
Approved for public release; distribution is unlimited.

13. SUPPLEMENTARY NOTES

14. ABSTRACT
The analytical theories that describe the irradiance profile and scintillation index for a Gaussian beam propagating through atmospheric turbulence are reviewed. Both horizontal and slant propagation paths are considered. A turbulence strength C_n^2 model, with daytime and nighttime versions, is described that is generally consistent with our understanding of White Sands Missile Range (WSMR), NM conditions. The expressions and turbulence strength model are used to generate a set of curves that show received beam sizes and scintillation indices as a function of the initial beam size (radius), the wavelength, the path elevation angle, and the propagation distance.

15. SUBJECT TERMS
Laser propagation, turbulence, optical, transmission, beam size

16. SECURITY CLASSIFICATION OF:			17. LIMITATION OF ABSTRACT	18. NUMBER OF PAGES	19a. NAME OF RESPONSIBLE PERSON
a. REPORT	b. ABSTRACT	c. THIS PAGE			Dr. Joseph Montoya
U	U	U	UU	26	19b. TELEPHONE NUMBER (*Include area code*) (575) 678-5551

Standard Form 298 (Rev. 8/98)
Prescribed by ANSI Std. Z39.18

Contents

List of Figures

Preface

For many applications involving laser irradiance on a target, there exists a limitation on intensity because of atmospheric effects. One of the main atmospheric influences is the effect due to the change in index of refraction caused by temperature gradients on the order of 0.1 to 1° C. In 2007, the U.S. Army Research Laboratory (ARL) Survivability/Lethality Analysis Directorate (SLAD), White Sands Missile Range (WSMR), NM decided to investigate this effect with Dr. Voelz, a faculty member at New Mexico State University (NMSU), Las Cruces, NM. Dr. Voelz has extensive experience with atmospheric turbulence effects and the propagation of light through turbulent media. Other effects that are caused by propagation through the atmosphere include absorption, scattering, and high power laser effects such as blooming. However, the effect of turbulence was the main consideration in this report. The NMSU group applied both analytic expressions and propagation modeling tools in order to derive the intensity profile at the target area. Various propagation distances as well as initial beam exit apertures were considered. The wavelength range and the propagation angle were also varied. Specific parameters related to location and turbulence strength were supplied as needed. This effort fills a gap in the existing data already available for the propagation of laser light through turbulence and the resulting intensity profiles. Dr. Joseph Montoya, of ARL/SLAD, created the statement of work and gave guidance at various times during the project.

INTENTIONALLY LEFT BLANK.

1. Introduction

For many applications involving laser propagation through the atmosphere, there exists a limitation on the received flux because of atmospheric effects. One of the main atmospheric influences is the effect due to the change in index of refraction caused by temperature gradients on the order of 0.1 to 1° C. These gradients comprise the effect known as turbulence, which increases the beam divergence and creates a temporal variation of the beam irradiance at a receiver. This variation is commonly termed "scintillation". For many communication and remote sensing applications, a beam needs to be transmitted near the Earth's surface along a path that is horizontal or has a slight incline to the surface. This inclined path, or "slant" path, involves the transit of the beam through varying turbulence strengths at different altitudes above the surface.

In this report, we list the currently favored analytical expressions that describe the irradiance profile and scintillation index for a Gaussian beam propagating through turbulence. These expressions have been applied extensively to free-space laser communications and other beam pointing applications. The turbulence strength C_n^2 model (daytime and nighttime versions), is also discussed and is generally consistent with our understanding of the conditions at White Sands Missile Range (WSMR), NM. The expressions and turbulence strength model are used to generate a set of plots and curves that show the received beam size and scintillation index as a function of the initial beam size (radius) w_0, the wavelength λ, the path elevation angle θ, and the propagation distance. The range of values considered are as follows: w_0 (2.5 to 10 in.), λ (0.5 to 5 μm), θ (0 to 40°), and distance, or range (0 to 20 km). The curves can be used to determine the expected beam size and scintillation index for various horizontal and slant path situations.

2. Analytical Expressions

Figure 1 shows a schematic diagram for a laser beam propagating through the atmosphere to a target along (a) a horizontal path, and (b) a slant path. Consider a Gaussian beam with the optical field of unit amplitude written as

$$U(x,y) = \exp\left(-\frac{x^2+y^2}{w_0^2}\right), \tag{1}$$

where w_0 defines the initial beam size (e^{-1} field radius), x and y are the horizontal and vertical coordinates of the incident beam field from the beam center, respectively. As the Gaussian beam propagates over a distance L, the characteristics of the received beam have been carefully described by Andrews and Phillips (*1, 2*). The relevant expressions for the horizontal and slant propagations are now reviewed.

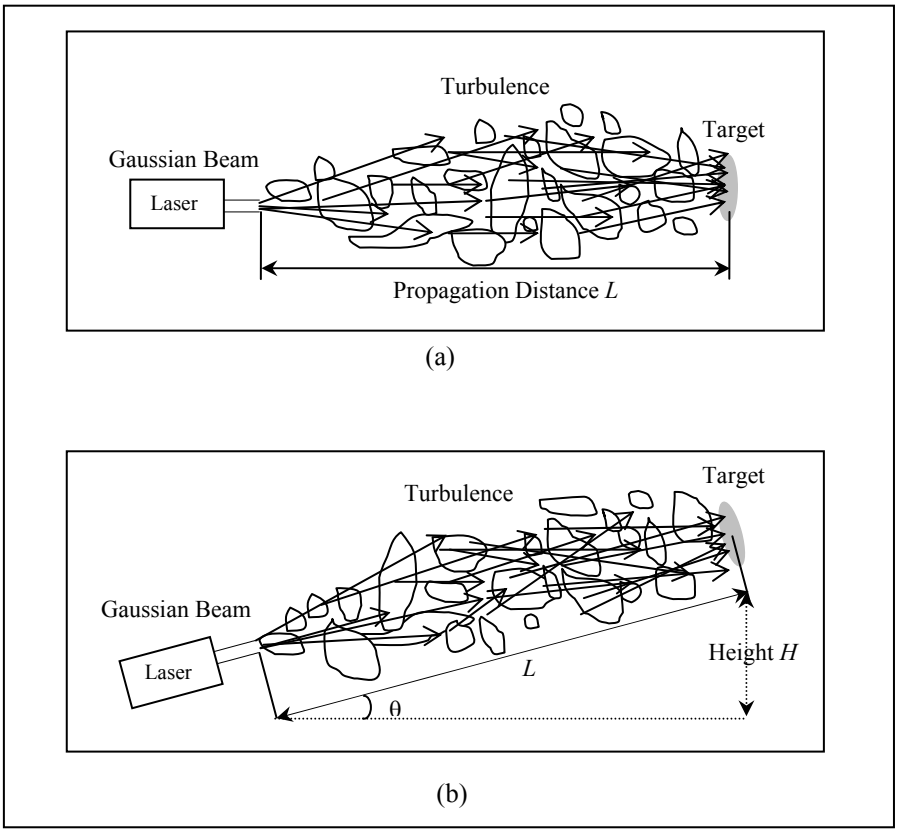

Figure 1. Schematic diagram of a Gaussian beam propagating through turbulence along a (a) horizontal and (b) slant path.

2.1 Horizontal Propagation

2.1.1 Intensity Profile

The irradiance (often referred to as intensity) function of the beam at a distance L from the source can be expressed by

$$I(x, y, L) = \frac{w_0^2}{w(L)^2} \exp\left[-\frac{2(x^2 + y^2)}{w(L)^2}\right], \tag{2}$$

where $w(L)$ is the average beam size (radius) at the receiver given by

$$w(L) = w_0 \left[1 + \left(\frac{2L}{k w_0}\right)^2\right]^{1/2} \left[1 + 1.63 \sigma_R^{12/5} \Lambda(L)\right]^{1/2}, \tag{3}$$

where $k = 2\pi/\lambda$ and λ is the wavelength of the beam, σ_R^2 is the Rytov variance, and $\Lambda(L)$ is the Fresnel ratio for vacuum propagation.

The Rytov variance σ_R^2 is the variance of the log-irradiance fluctuations of the field. It generally signifies "weak" turbulence (phase dominated effects) if it has a value less than 1, and "medium-to-strong" turbulence if greater than 1. If the turbulence strength along a horizontal path is assumed to be constant then the Rytov variance can be expressed as

$$\sigma_R^2(L) = 1.23 C_n^2 k^{\frac{7}{6}} L^{\frac{11}{6}}, \tag{4}$$

where C_n^2 is the turbulence structure constant that characterizes the strength of the index of refraction fluctuations. Equation 4 assumes a Kolomogorov turbulence spectrum. Note that the Rytov variance is directly proportional to the turbulence strength, approximately inversely proportional to the wavelength and approximately proportional to the propagation distance squared.

The Fresnel ratio $\Lambda(L)$ in equation 3, characterizes the beam spread due to diffraction for vacuum propagation. $\Lambda(L)$ is associated with the beam curvature parameter $\Theta(L)$, which describes the phase curvature of the beam as it propagates in vacuum. These parameters are dependent on the initial Fresnel ratio $\Lambda_0(L)$ and curvature parameter $\Theta_0(L)$ that include the initial beam size and curvature at the transmit plane. The key relationships are as follows:

$$\Theta(L) = \frac{\Theta_0(L)}{\Theta_0^2(L) + \Lambda_0^2(L)}, \tag{5}$$

$$\Lambda(L) = \frac{\Lambda_0(L)}{\Theta_0^2(L) + \Lambda_0^2(L)}, \tag{6}$$

$$\Theta_0(L) = 1 - \frac{L}{F_0}, \tag{7}$$

$$\Lambda_0(L) = \frac{2L}{k \cdot w_0^2}, \tag{8}$$

where F_0 is the (phase) curvature of the beam at the transmitter. For a Gaussian beam F_0 is usually assumed to be infinite, so $\Theta_0(L) = 1$.

2.1.2 Scintillation Index

The scintillation index is defined as the normalized variance of the irradiance fluctuations at a receiver, that is,

$$\sigma_I^2(x,y,L) = \frac{\left\langle I^2(x,y,L)\right\rangle - \left\langle I(x,y,L)\right\rangle^2}{\left\langle I(x,y,L)\right\rangle^2}, \tag{9}$$

where I is the irradiance, x and y are transverse coordinates at the receiver, and L is again the propagation distance. Scintillation index expressions are commonly separated into two forms: one for "weak" fluctuation conditions and one for "strong" fluctuation conditions. As previously noted, the test for these conditions involves the Rytov variance.

Based on a Kolmogorov turbulence spectrum, the scintillation index at the beam's center point for a weak turbulence case can be expressed as

$$\sigma_{I,w}^2(x,y,L) = 3.86\sigma_R^2\ \mathrm{Re}\left[i^{\frac{5}{6}} F\left(\overline{\Theta}(L) + i\Lambda(L)\right) - \frac{11}{6}\left(\Lambda(L)\right)^{\frac{5}{6}} \right], \tag{10}$$

where $F(\ldots)$ is a hypergeometric function (1), $\overline{\Theta}(L)$is equal to 1- $\Theta(L)$ and i is the imaginary unit. For a Gaussian beam, the initial beam curvature F_0 is ∞, and equation 10 becomes

$$\sigma_{I,w}{}^2 = 3.86\sigma_R^2 \left\{ 0.4\left[\left(1+2\Theta(L)\right)^2 + 4\left(\Lambda(L)\right)^2\right]^{\frac{5}{12}} \cos\left[\frac{5}{6}\tan^{-1}\left(\frac{1+2\Theta(L)}{2\Lambda(L)}\right)\right] - \frac{11}{16}\left(\Lambda(L)\right)^{\frac{5}{6}} \right\}. \tag{11}$$

Under medium-to-strong turbulence conditions, the scintillation index $\sigma_{I,s}{}^2$ is given by

$$\sigma_{I,s}{}^2 = \exp\left[\frac{0.49\sigma_{I,w}{}^2}{\left(1+0.56\sigma_{I,w}{}^{\frac{12}{5}}\right)^{\frac{7}{6}}} + \frac{0.51\sigma_{I,w}{}^2}{\left(1+0.69\sigma_{I,w}{}^{\frac{12}{5}}\right)^{\frac{5}{6}}} \right] - 1, \tag{12}$$

where the scintillation index for the weak case $\sigma_{I,w}{}^2$ is applied in equation 12 to determine the result for the medium-to-strong case.

2.2 Slant Path

2.2.1 Intensity Profile

For Gaussian beam propagation through turbulence over a slant path of length L, the expression of the received beam size is generally the same as equation 3. However, in this situation, the path is characterized by the elevation angle θ (i.e., the angle of beam with respect to the horizontal direction), and the height change H between the transmitter and receiver. For an upward slant path, the relationship between these parameters can be easily obtained from the geometry in figure 1(b):

$$H = L \sin\theta \,. \tag{13}$$

Because the beam height changes along the propagation path and the turbulence strength C_n^2 is a function of height, the Rytov variance is modified to the following form

$$\sigma_R^2 = 2.25 k^{\frac{7}{6}} H^{\frac{5}{6}} (\sin\theta)^{-\frac{11}{6}} \int_{h_0}^{H+h_0} C_n^2(h) \cdot \left(1 - \frac{h-h_0}{H}\right)^{\frac{5}{6}} dh \,, \tag{14}$$

where $C_n^2(h)$ indicates the turbulence strength as a function of height h from the ground and h_0 is the initial height of the beam transmitter. Substituting equation 14 into equation 3 gives an expression for the beam size for the upward slant path propagation.

2.2.2 Scintillation Index

The expressions within the curly bracket of equation 11 involve only the parameters Θ and Λ, which are functions of propagation distance L, but are independent of the turbulence parameters. Consequently, the Rytov variance σ_R^2 is the only parameter affected by the slant path turbulence (*2*). Using equation 14 with equation 11, leads to an expression for the scintillation index for slant path propagation under weak turbulence. The scintillation index for medium-to-strong turbulence is again given by equation 12.

---

3. C_n^2 Profiles

The C_n^2 profile is the key function that characterizes the turbulence strength with height. Information provided by WSMR personnel suggested that typical daytime conditions at WSMR can be modeled with a –4/3 height dependence near the ground and nighttime conditions involve a –2/3 dependence. A C_n^2 profile published by Comeron et al., matches these conditions; therefore, we used this profile for the results presented in this report (*3*).

The expression used for the height dependence of C_n^2 for daytime conditions is

$$C_n^2(h) = \begin{cases} C_{n0}^2 \left(\frac{h_s}{h_0}\right)^{-\frac{4}{3}} \exp\left(-\frac{h_s}{h_r}\right) \exp\left(\frac{h_0}{h_r}\right) \cdot \left(\frac{h}{h_s}\right)^{-\frac{2}{3}}, & \text{if } h < h_s \\ C_{n0}^2 \left(\frac{h}{h_0}\right)^{-\frac{4}{3}} \exp\left(\frac{h_0}{h_r}\right) \exp\left(-\frac{h}{h_r}\right) + C_{n1}^2 \exp\left(-\frac{h}{h_1}\right) & \\ \quad + C_{n1}^2 3 w_1^2 \left(\frac{h}{h_t}\right)^{10} \exp\left(-\frac{10h}{h_t}\right), & \text{otherwise} \end{cases} \tag{15}$$

where the surface layer height h_s is 4 m and the reference height h_0 is 8 m. The height marking the fall-off of the $h^{-4/3}$dependence h_r is 100 m, the height above the terrain is h, and the height characterizing the exponential fall-off of the structure constant in the free-atmosphere region h_1 is 1500 m. The tropopause height h_t is 13,000 m; the root mean squared wind velocity averaged over the 5 to 20 km altitude interval w_1 is 30 m/s; the structure constant in the zone with $h^{-4/3}$ dependence is $C_{n0}^2 = 1.7\text{x}10^{-13}$ m$^{-2/3}$; and the structure constant value for free atmosphere is $C_{n1}^2 = 10^{-16}$ m$^{-2/3}$.

The expression used for the height dependence of C_n^2 for nighttime conditions is

$$C_n^2(h) = \begin{cases} C_{n0}^2 \left(\frac{h}{h_s}\right)^{-\frac{2}{3}}, & \text{if } h \le h_s \\ C_{n0}^2, & \text{if } h_s < h < h_i \\ C_{n0}^2 \exp\left(\frac{h_i}{h_r}\right) \exp\left(-\frac{h}{h_r}\right) + C_{n1}^2 \exp\left(-\frac{h}{h_l}\right) + C_{n1}^2 3 w_1^2 \left(\frac{h}{h_t}\right)^{10} \exp\left(-\frac{10h}{h_t}\right), & \text{if } h > h_i \end{cases} \tag{16}$$

where h_i =30 m, $C_{n0}^2 = 9.5\times10^{-15}m^{-2/3}$, and $C_{n1}^2 = 4.5\times10^{-17}m^{-2/3}$. Figure 2 presents a plot of the logarithm of the C_n^2 profile for day- and nighttime conditions. It is clear that from the ground up to about 100 m the daytime turbulence is significantly stronger than nighttime turbulence.

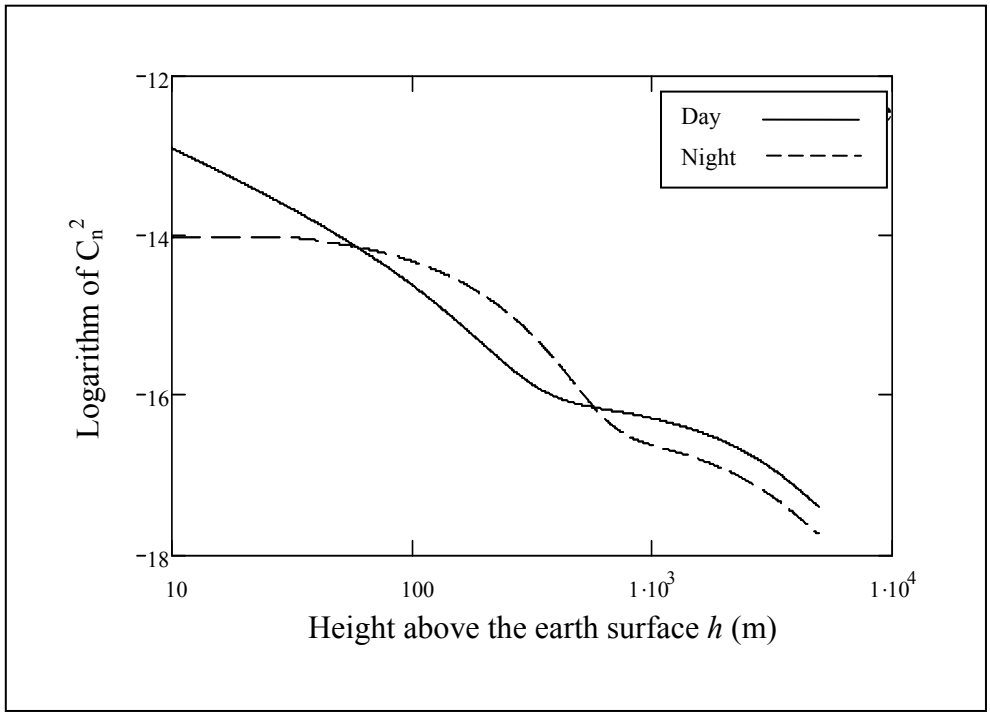

Figure 2. Daytime and nighttime C_n^2 profiles used in this report (*3*).

4. Results and Discussions

4.1 Beam Size

For our calculations, the initial height of the laser transmitter h_0 was assumed to be 8 m. A set of curves for the beam size as a function of propagation distance L, elevation angle θ, initial Gaussian beam size w_0, wavelength λ, and different C_n^2 profiles are shown in figures 3 through 6. Observations regarding these results are as follows:

1. For horizontal propagation, the beam size is driven by the atmospherics so wavelength and initial beam size have little effect on the beam divergence where the turbulence is most severe.
2. Diffraction limited spreading becomes more of a factor for the slant path cases where the turbulence is less severe, thus the wavelength and initial beam size become more important.
3. Beam spread is somewhat larger during the day than at night, but the change in size between these two cases is not substantial.

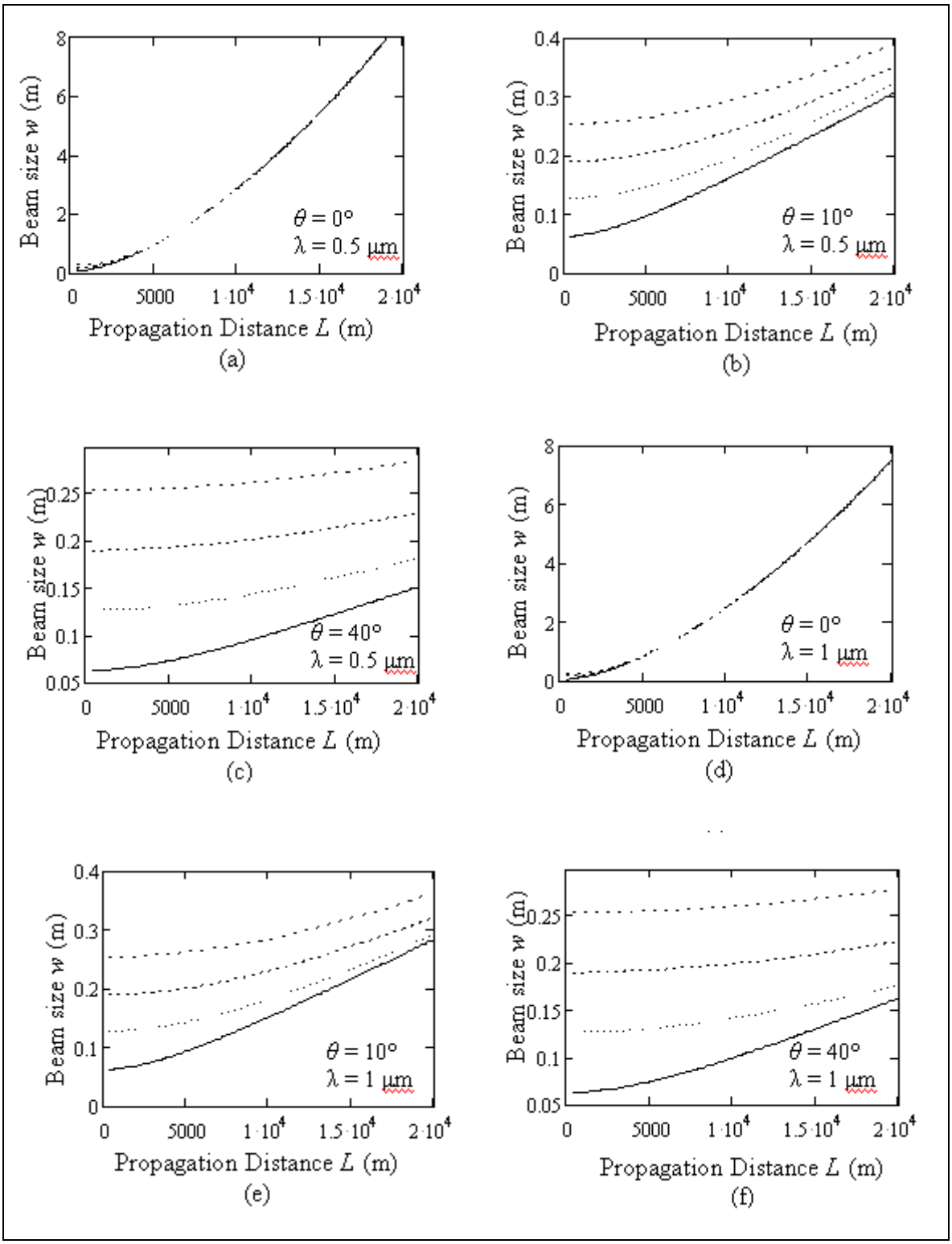

Figure 3. Beam size w(L) for the slant path propagation of a Gaussian beam versus propagation distance L in the daytime.

Note: λ = 0.5 μm in (a), (b), and (c), 1 μm in (d), (e), and (f), elevation angle θ = 0°, 10, 40°, and initial Gaussian beam size w_0 = 2.5 in. (solid), 5 in. (dot), 7.5 in. (dash), and 10 in. (dash-dot).

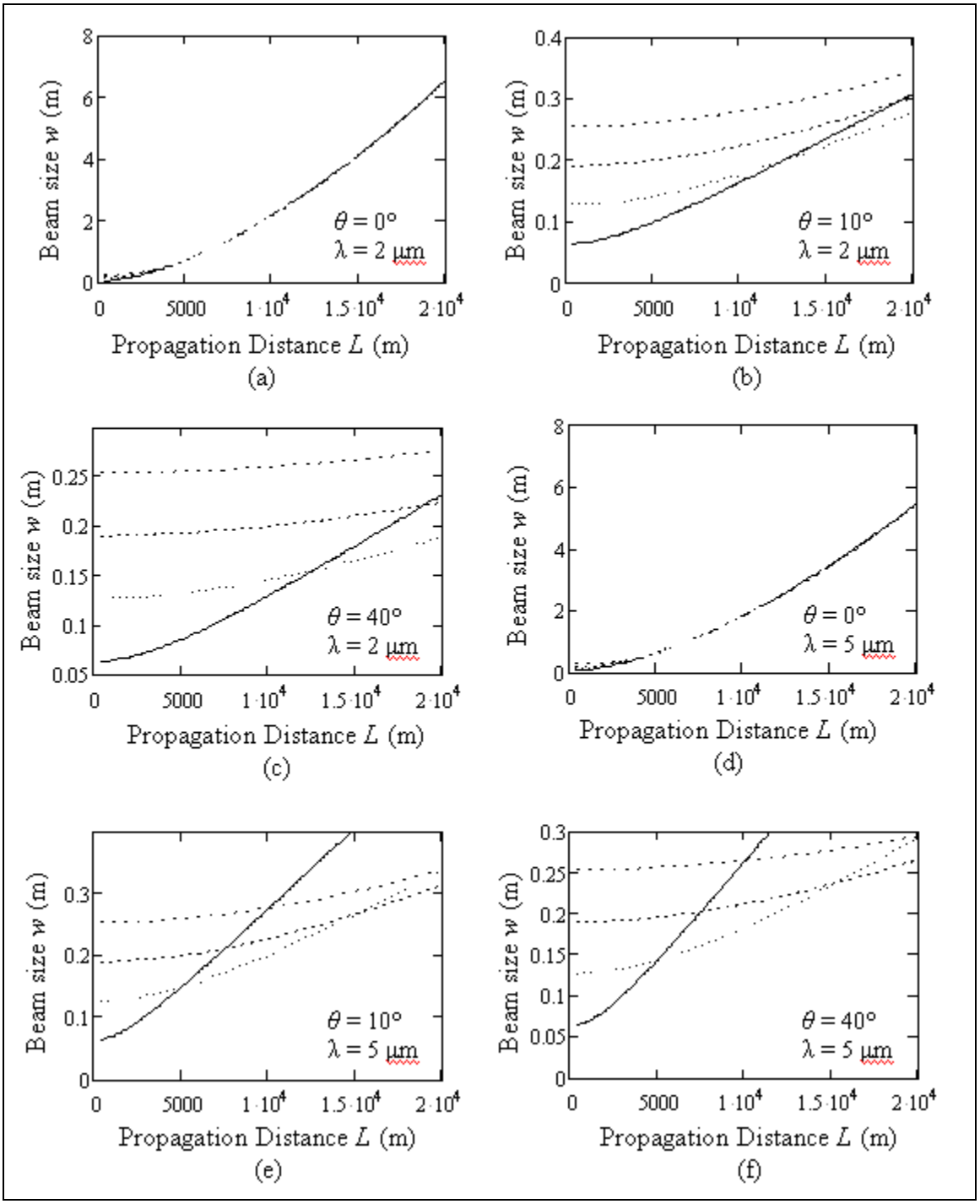

Figure 4. Beam size $w(L)$ for the slant path propagation of a Gaussian beam versus propagation distance L in the daytime.

Note: with $\lambda = 2$ μm in (a), (b), and (c), 5 μm in (d), (e), and (f), elevation angle $\theta = 0°$, 10, 40°, and initial Gaussian beam size $w_0 = 2.5$ in. (solid), 5 in. (dot), 7.5 in. (dash), and 10 in. (dash-dot).

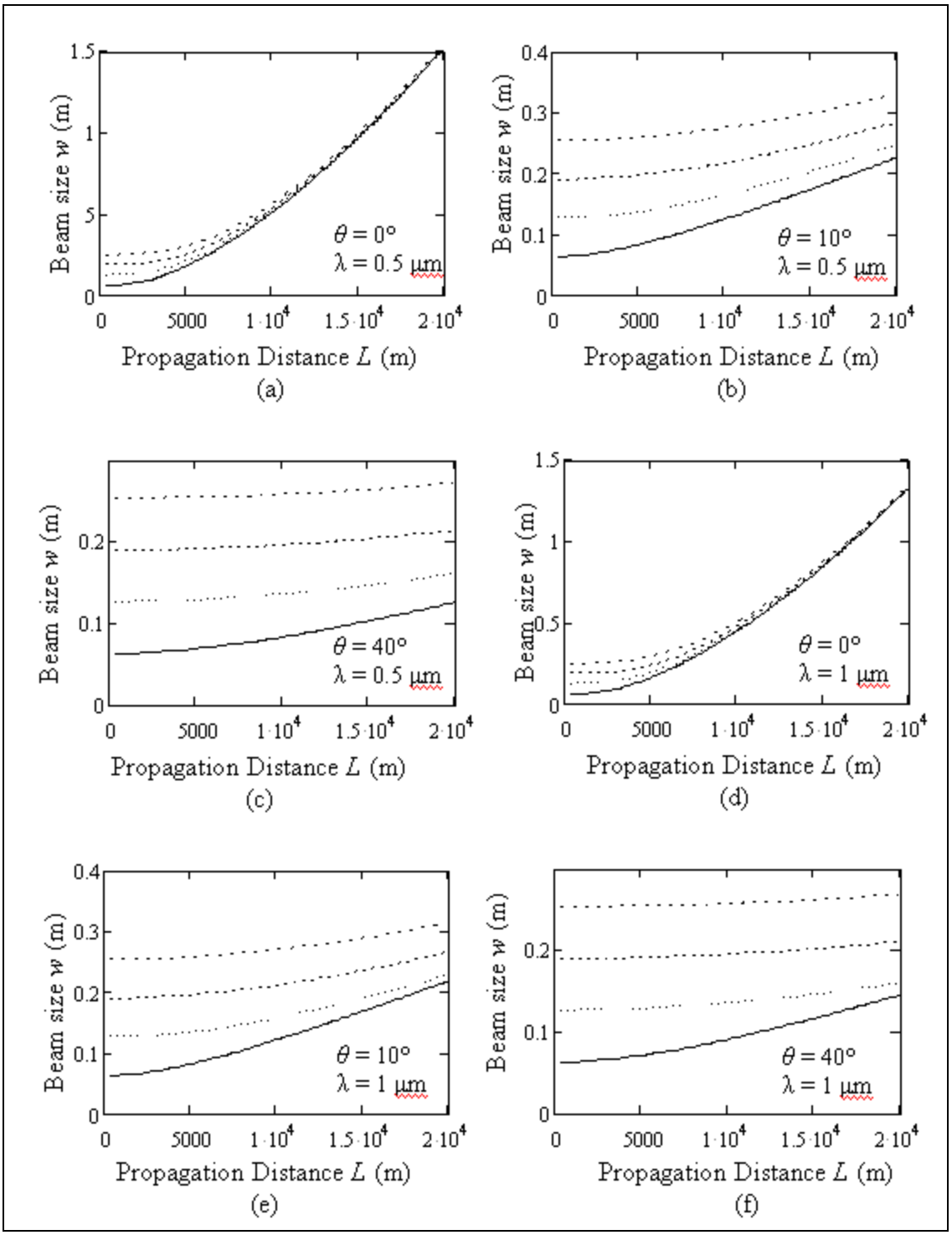

Figure 5. Same as figure 3, except in the nighttime.

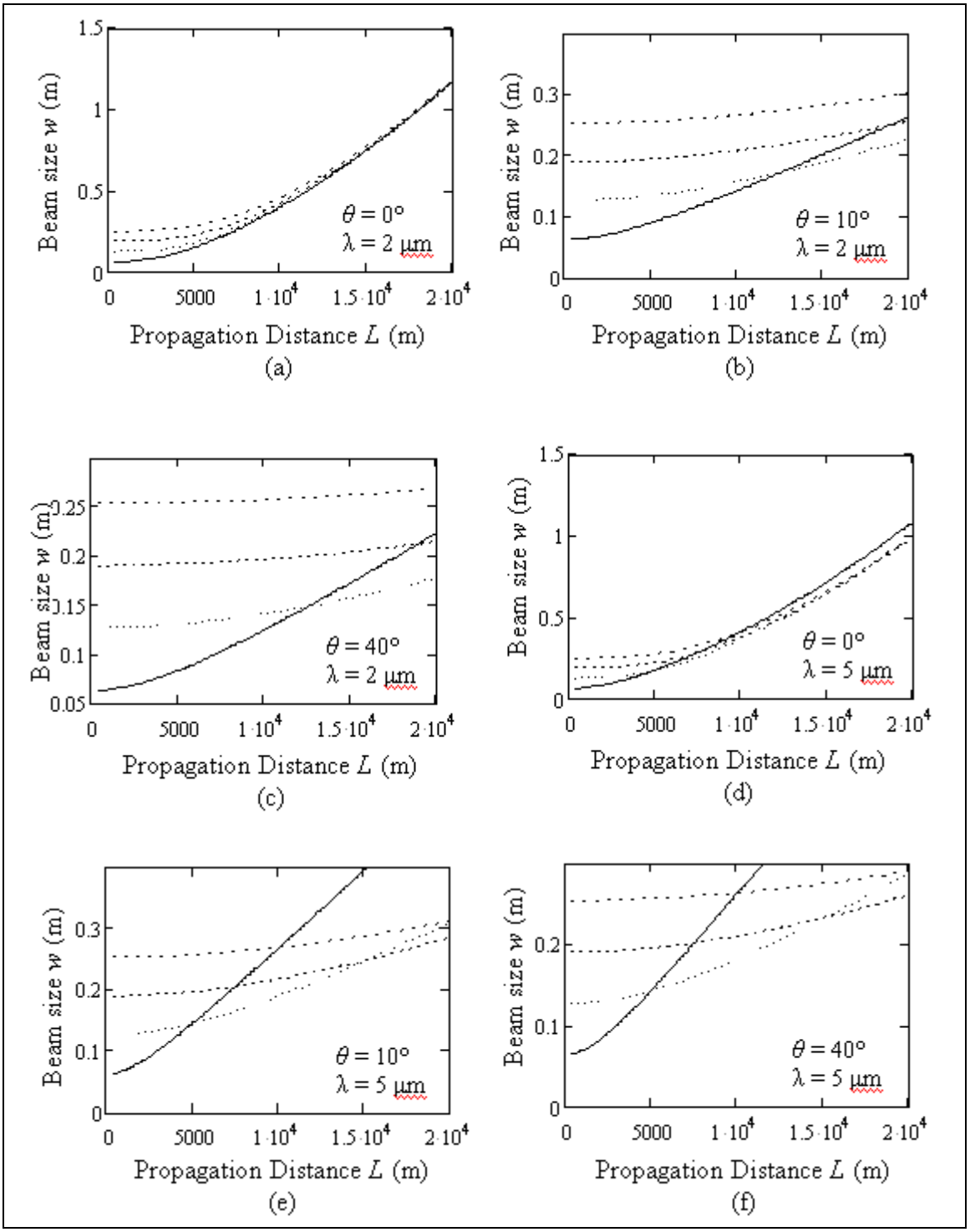

Figure 6. Same as figure 4, except in the nighttime.

4.2 Scintillation Index

A set of curves for the scintillation index are presented in figures 7 through 10. The observations on these results are as follows:

1. As expected, longer wavelengths and higher elevation angles generally result in lower scintillation.
2. For horizontal propagation, the scintillation index saturates (at a value of ~1.7) for all wavelengths and initial beam sizes within the 20 km distance, although the shortest wavelengths reach saturation with propagation lengths of less than 1 km.
3. For the slant paths, the smaller initial beam sizes result in somewhat less scintillation.

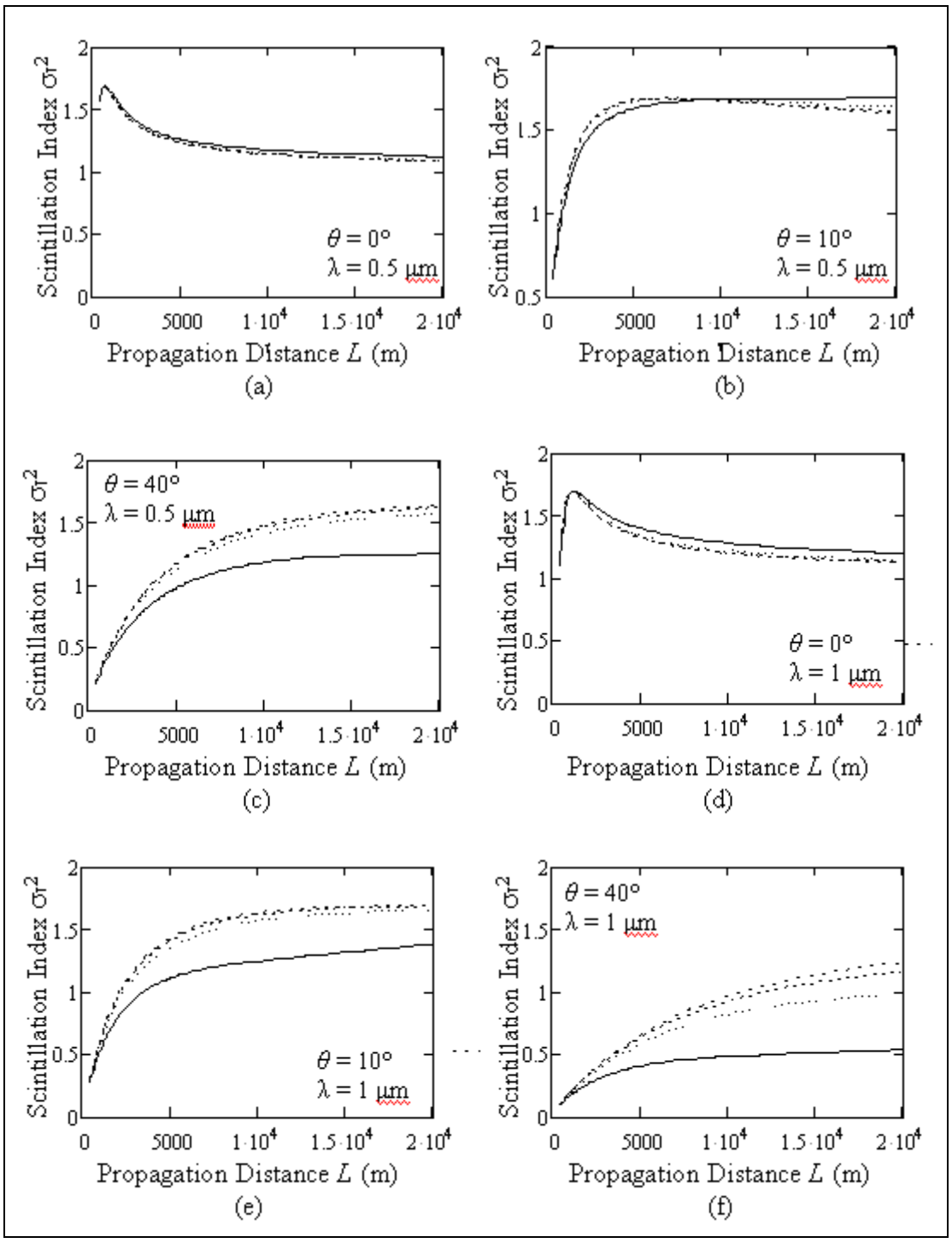

Figure 7. Scintillation index versus propagation distance L during daytime.

Note: $\lambda = 0.5$ μm in (a), (b), and (c), 1 μm in (d), (e), and (f), elevation angle $\theta = 0°$, 10, 40°, and initial Gaussian beam size $w_0 = 2.5$ in. (solid), 5 in. (dot), 7.5 in. (dash), and 10 in. (dash-dot).

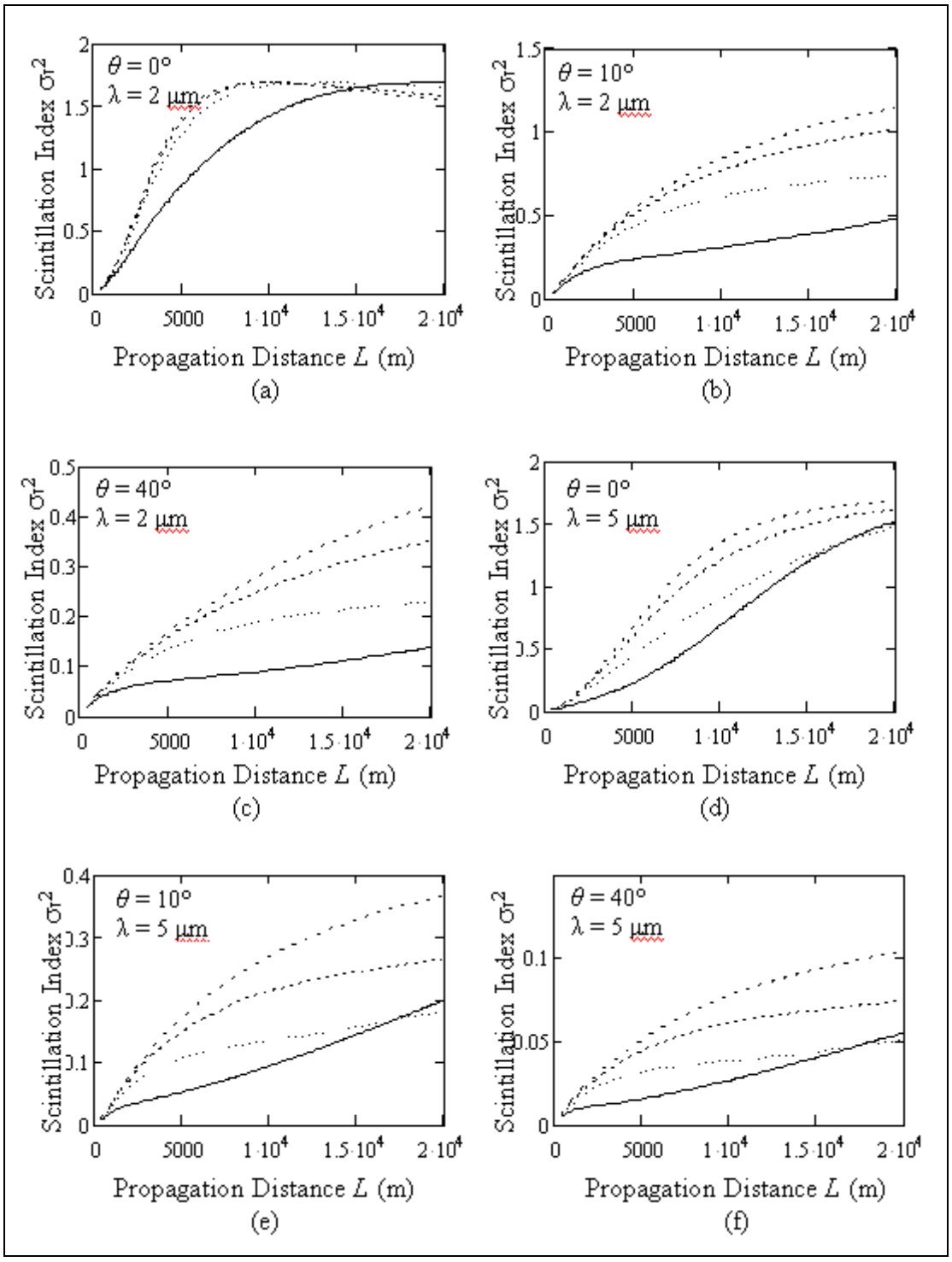

Figure 8. Scintillation index versus propagation distance L in the nighttime.

Note: $\lambda = 2$ μm in (a), (b), and (c), 5 μm in (d), (e), and (f), elevation angle $\theta = 0°$, 10, 40°, and initial Gaussian beam size $w_0 = 2.5$ in. (solid), 5 in. (dot), 7.5 in. (dash), and 10 in. (dash-dot).

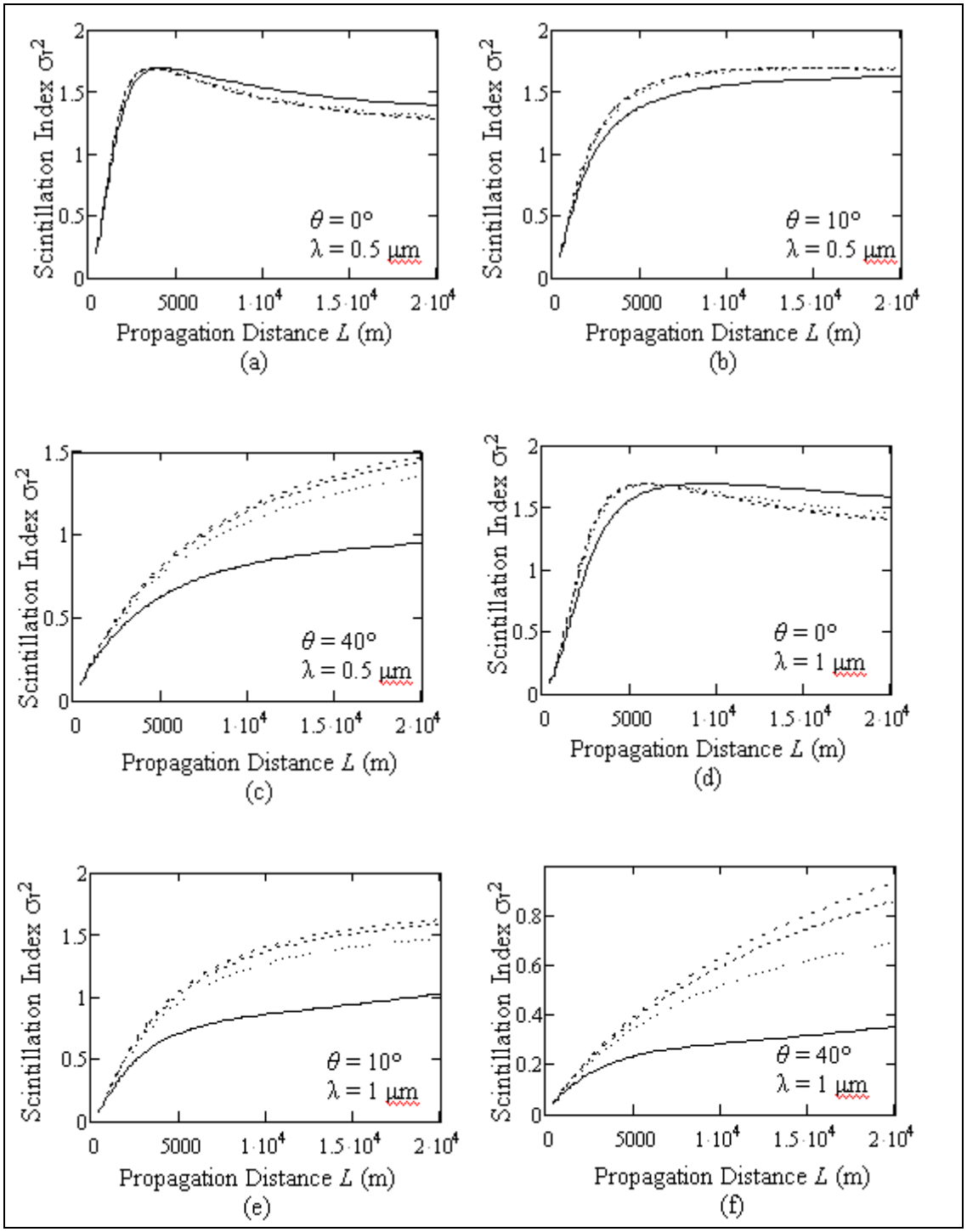

Figure 9. The same as figure 7, except in the nighttime.

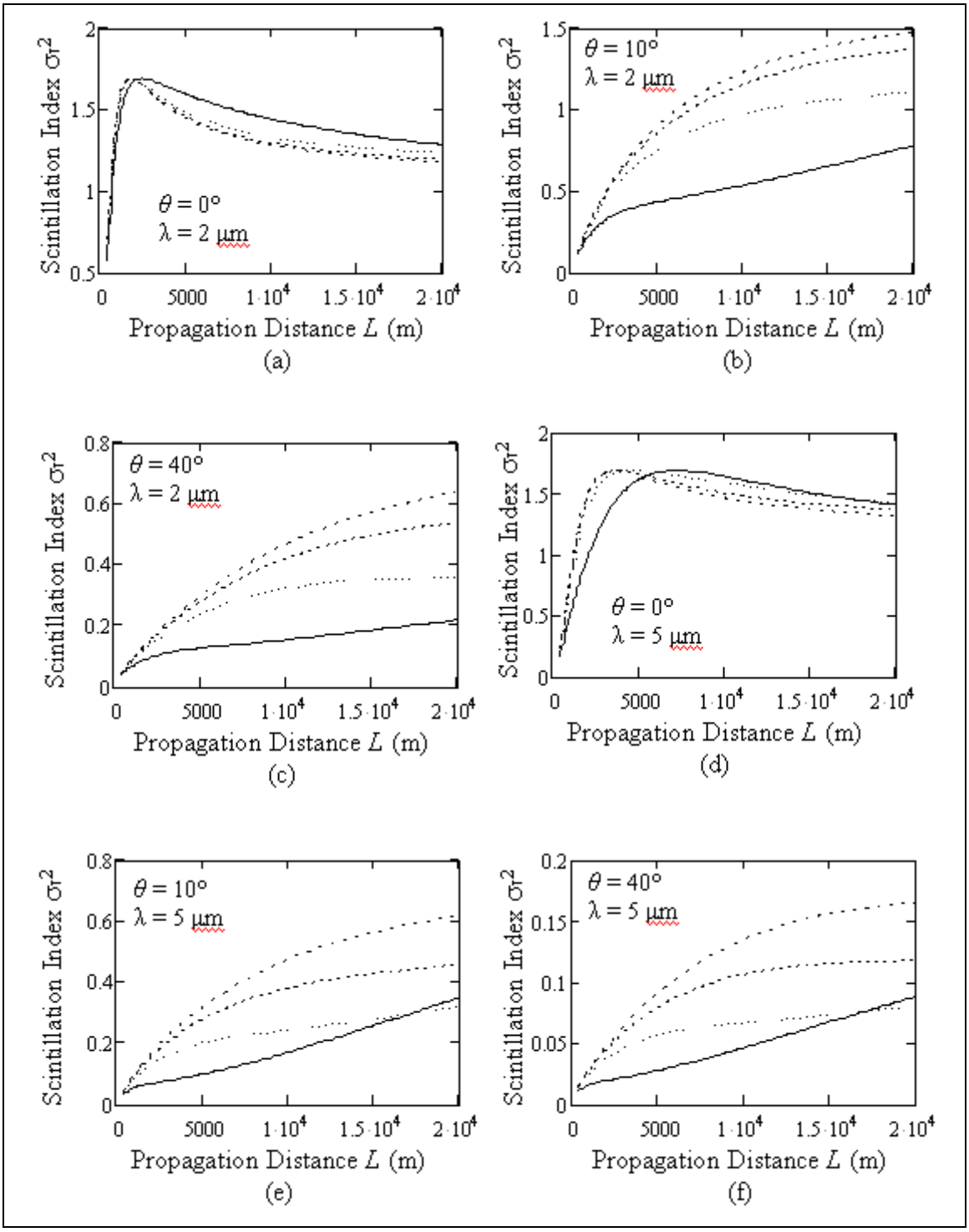

Figure 10. The same as figure 8, except in the nighttime.

5. Concluding Remarks

The curves provided in this report are adequate for first-order estimates of beam size and scintillation index for the parameter space that was investigated. Some of the results were spot-checked with results from wave optics simulations and were found in good agreement. In regard to beam size, there are some indications from our wave optics simulation work, that beam size in strong turbulence may be overestimated by the analytic theory applied in this report. There may be a saturation effect that is not being considered; therefore, this issue requires further investigation. We emphasize that scintillation index values are computed only for the center of the received beam and normalized intensity fluctuations near the beam edges will tend to be larger. Furthermore, the effect of beam wander is not fully characterized in the analytic expressions used in this report (*4*). Beam wander becomes important in situations where the beam is generally tilted rather than broken up by turbulence. Beam wander may tend to increase the scintillation values for some of the slant path cases. We did not investigate the temporal characteristics of the scintillation, which depend on a variety of factors such as wind speed. This could be examined in the future. Finally, we emphasize that our results are dependent on the assumed C_n^2 profile, although most commonly accepted profiles should produce similar results.

References

1. Andrews, L. C.; Phillips, R. L.; Hopen, C. Y. *Laser Beam Scintillation with Applications*; SPIE Optical Engineering Press: Bellingham, WA, 2001.
2. Andrews, L. C. *Field Guide to Atmospheric Optics*; SPIE Optical Engineering Press: Bellingham, WA, 2002.
3. Comeron, A.; Dios, F.; Rodriguez, A.; Rubio, J. A.; Reyes, M.; Alonso, A. Modeling of power fluctuations induced by refractive turbulence in a multiple-beam ground-to-satellite optical uplink. *Proceedings of the SPIE*, 5892, August 2005.
4. Chu, X.; Liu, Z.; Y. Wu. Propagation of a general multi-Gaussian beam in turbulent atmosphere in a slant path. *J. Opt. Soc. Am*. **2008**, A 25, 1, 74–79.

No. of Copies	Organization
1 PDF	ADMNSTR DEFNS TECHL INFO C ATTN DTIC OCP 8725 JOHN J KINGMAN RD STE 0944 FT BELVOIR VA 22060-6218
1 CD	US ARMY RSRCH LAB ATTN AMSRD ARL CI OK TP TECHL LIB T LANDFRIED BLDG 4600 APG MD 21005-5066
3 CDs	US ARMY RSRCH LAB ATTN AMSRD ARL CI OK T TECHL PUB ATTN AMSRD ARL CI OK TL TECHL LIB ATTN IMNE ALC IMS MAIL & RECORDS MGMT ADELPHI MD 20783-1197
2 CDs	US ARMY RESEARCH LAB IEPD CHIEF A R FLORES ATTN AMSRD ARL SL E WSMR NM 88002-5513
6 CDs	US ARMY RESEARCH LAB INFO & ELEC PROTECTION DIV ATTN AMSRD ARL SL EG J MONTOYA WSMR NM 88002-5513

Total: 13 (1 PDF, 12 CDs)

INTENTIONALLY LEFT BLANK.